ACS OMEGA

Open Access

http://pubs.acs.org/journal/acsodf

Article

Thermodynamic H-Abstraction Abilities of Nitrogen Centered Radical Cations as Potential Hydrogen Atom Transfer Catalysts in Y−H Bond Functionalization

Xia Zhao, Yi-Lin Hou, Bao-Chen Qian,* and Guang-Bin Shen*

Cite This: *ACS Omega* 2024, 9, 26708−26718

Read Online

ACCESS | Metrics & More | Article Recommendations | Supporting Information

ABSTRACT: Y−H bond functionalization has always been the focus of research interest in the area of organic synthesis. Direct hydrogen atom transfer (HAT) from the Y−H bond is one of the most efficient and practical methods to activate the Y−H bond. Recently, nitrogen centered radical cations were broadly utilized as H-abstraction catalysts to activate Y−H bonds via the HAT process. As a type of HAT catalyst, the H-affinity of nitrogen centered radical cations is a significant thermodynamic parameter to quantitatively evaluate the thermodynamic H-abstraction potentials of nitrogen centered radical cations. In this work, the pK_a values of 120 protonated N-containing compounds in acetonitrile (AN) are predicted, and the H-affinities of 120 nitrogen centered radical cations in AN are derived from the reduction potentials of nitrogen centered radical cations and pK_a of protonated N-containing compounds using Hess' law. This work focuses on the H-abstraction abilities of 120 nitrogen centered radical cations in AN to enrich the molecule library of novel HAT catalysts or H-abstractors and provides valuable thermodynamic guidelines for the application of nitrogen centered radical cations in Y−H bond functionalization.

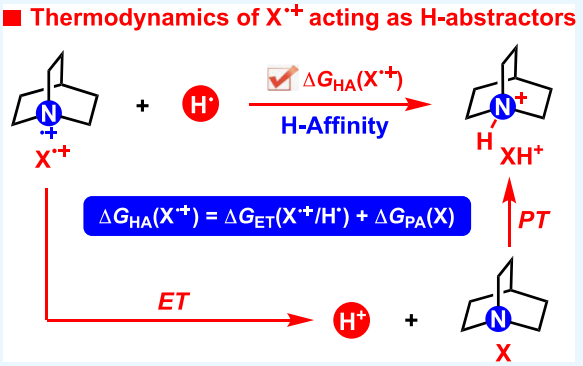

1. INTRODUCTION

Y−H bond functionalization,[1,2] especially for a C−H bond,[3−6] has always been the focus of research interest in the area of organic synthesis. Many synthetic strategies were developed to activate a Y−H bond into Y•, such as Y−H activation by metal catalysts,[7−9] H-abstraction by hydrogen atom transfer (HAT) catalysts[10−16] or oxidative multisite proton-coupling electron transfer (ET) (MS-PCET) reagents,[17−23] etc. Among so many activation methods, direct HAT from the Y−H bond is one of the most efficient and practical methods, in which HAT is one of the key steps in a wide variety of Y−H functionalization reactions.[10−16] Recently, nitrogen centered radical cations ($X^{\bullet+}$) were broadly applied as H-abstraction reagents to activate the Y−H bond via the HAT process.[12−15,24−43] A typical reaction mechanism of the triple catalytic radical reactions involving $X^{\bullet+}$ acting as HAT catalysts is shown in Scheme 1.[27−32]

From Scheme 1, it is clear that $X^{\bullet+}$, generated from the single electron transfer between excited photocatalyst (*PC) and nitrogen containing substrate X (*PC + X → $PC^{\bullet-}$ + $X^{\bullet+}$), are potential HAT catalysts in Y−H bond functionalization, and one of the key elementary steps is the HAT from Y−H bond to $X^{\bullet+}$ producing the Y•. The reactive Y• experiences following radical addition or substitution processes.[27−32] In practice, $Et_3N^{\bullet+}$ (**15**$^{\bullet+}$),[33−35] quinuclidine radical cation (1-azabicyclo[2.2.2]octane radical cation, $ABCO^{\bullet+}$ or **21**$^{\bullet+}$),[27−32] $DABCO^{\bullet+}$ (1,4-diazabicyclo[2.2.2]octane radical cation, **23**$^{\bullet+}$),[36−39] aniline radical cation (**26**$^{\bullet+}$),[40,41] and pyridine radical cation (**70**$^{\bullet+}$)[42,43] were often reported as HAT catalysts or H-abstractors in chemical reactions (Scheme 1).

Therefore, as a type of efficient HAT catalyst or H-abstractor, the hydrogen atom affinity (H-affinity) of $X^{\bullet+}$ is a significant thermodynamic parameter to quantitatively measure the thermodynamic H-abstraction reactivity of an $X^{\bullet+}$ and provide valuable guidelines for the application of $X^{\bullet+}$ in Y−H bond functionalization.[27−43] It is well-known that nitrogen centered radical cations ($X^{\bullet+}$) are highly active intermediates. Considering the stability, possible side effects, and resulting concentration of $X^{\bullet+}$, the H-affinities of $X^{\bullet+}$ could not be directly measured by isothermal titration calorimetry or other bond energy measurement methods. In this work, the pK_a values of 120 XH^+ (protonated N-containing compounds) in AN are predicted, and the H-affinities of 120 $X^{\bullet+}$ are derived from the reduction potentials of $X^{\bullet+}$ and pK_a of XH^+ employing Hess' law by constructing a thermodynamic

Received: May 2, 2024
Revised: May 20, 2024
Accepted: May 23, 2024
Published: June 4, 2024

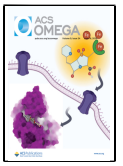

Scheme 1. Mechanism for the Triple Catalytic Radical Reactions Involving $X^{\bullet+}$ Functioning as HAT Catalysts

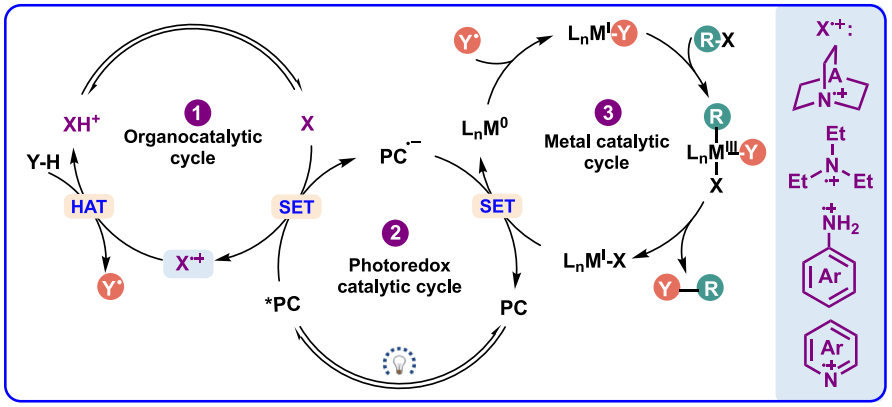

cycle.[44−46] Moreover, the thermodynamic H-abstraction properties of 120 $X^{\bullet+}$ (Scheme 2) in AN have been discussed in detail.

It should be noted that this work pays close attention to the thermodynamic potentials of $X^{\bullet+}$ abstracting hydrogen atoms and discusses the reactions feasibilities based on their thermodynamic driving forces. The thermodynamic values of the H-affinities for $X^{\bullet+}$ already reflect the steric and electronic effects from the molecular structures. However, the steric and electronic factors between $X^{\bullet+}$ and Y−H in the transition states have strong influences on the reactivities or reaction kinetics. Furthermore, different reactants ($X^{\bullet+}$ and Y−H) are involved in different HAT reactions, the reactivities are different, which is determined by the thermodynamic driving forces, temperature, solvents, steric effect, electronic effect, etc.[12] Among various effects, thermodynamic driving forces of HAT process are the important or decisive factor to determine the reaction rates or reactivities.[12] After evaluating the thermodynamic feasibilities of the HAT process, further kinetic study is efficient and meaningful. In all, the roles of steric and electronic effects are not factored into the thermodynamic analysis and can be considered a drawback of using this type of analysis; thus, these values can only provide thermodynamic guidance when considering a HAT catalyst. Therefore, the thermodynamic values of this work can only give thermodynamic guidance. The outcomes of catalytic reactions using such HAT agents are not predictable just based on the thermodynamic feasibility of the HAT event alone.[12] Factors such as polarity matching and steric hindrance (i.e., kinetic factor), electrophilicity, structural, and solvent effect of the HAT agent with its target substrate is also crucial in dictating reaction success/selectivity, which should be taken into consideration seriously after choosing a potential HAT agent.[12]

2. RESULTS AND DISCUSSION

Based on the chemical structures of frequently used nitrogen centered radical cations in Y−H functionalization, including $Et_3N^{\bullet+}$ (**15**$^{\bullet+}$),[33−35] quinuclidine radical cation (ABCO$^{\bullet+}$ or **21**$^{\bullet+}$),[27−32] DABCO$^{\bullet+}$ (**23**$^{\bullet+}$),[36−39] aniline radical cation (**26**$^{\bullet+}$),[40] *N*,*N*,*N*′,*N*′-tetramethyl-*p*-phenylenediamine radical cation (TMPA$^{\bullet+}$ or **32**$^{\bullet+}$),[41] and pyridine radical cation (**70**$^{\bullet+}$),[42,43] 120 $X^{\bullet+}$ of various structures are collected and evaluated in this work (Scheme 2). All of the 120 $X^{\bullet+}$ can be divided into four categories (Scheme 3), consisting of the general amine radical cations ($X_1^{\bullet+}$, **1**$^{\bullet+}$−**25**$^{\bullet+}$), aromatic amine radical cations ($X_2^{\bullet+}$, **26**$^{\bullet+}$−**53**$^{\bullet+}$), aromatic *N*-heterocycle radical cations ($X_3^{\bullet+}$, **54**$^{\bullet+}$−**83**$^{\bullet+}$), as well as tetra-substituted-hydrazine radical cations ($X_4^{\bullet+}$, **84**$^{\bullet+}$−**120**$^{\bullet+}$). It should be noted that 120 $X^{\bullet+}$ are not all centered on the actual nitrogen atom due to the existence of aromatic rings, such as $X_2^{\bullet+}$ and $X_3^{\bullet+}$. Since the final result is that N-centered radical cation abstracts a hydrogen atom to generate protonated product (XH^+), herein, nitrogen centered radical cations are used to take the place of radical cations derived from nitrogen-containing compounds for the convenience of description and understanding.

2.1. Definitions and Results of H-Affinity of $X^{\bullet+}$ in AN.

As for the chemical reaction of $X^{\bullet+}$ abstracting a hydrogen atom, the thermodynamic cycle (step 1−step 2−step 3) is constructed and shown in Scheme 4.

Step 1 is the chemical process of $X^{\bullet+}$ abstracting a hydrogen atom to generate XH^+, $X^{\bullet+} + H^{\bullet} \rightarrow XH^+$, and the thermodynamic H-abstraction ability of step 1 is described by the H-affinity of $X^{\bullet+}$, which is equal to the corresponding Gibbs free energy of $X^{\bullet+}$ abstracting a hydrogen atom: $\Delta G_{HA}(X^{\bullet+})$.[47]

Step 2 is the chemical process of ET from $H^{\bullet}$ to $X^{\bullet+}$, $X^{\bullet+} + H^{\bullet} \rightarrow X: + H^+$, and the thermodynamic driving force of step 2 is described by the Gibbs free energy of ET: $\Delta G_{ET}(X^{\bullet+}/H^{\bullet})$. $\Delta G_{ET}(X^{\bullet+}/H^{\bullet})$ could be computed by a combination of the oxidation potential of $H^{\bullet}$ and the reduction potential of $X^{\bullet+}$, $E_{ox}(H^{\bullet})$, and $E_{red}(X^{\bullet+})$, by eq 2 in Table 1, $\Delta G_{ET}(X^{\bullet+}/H^{\bullet}) = F[E_{ox}(H^{\bullet}) - E_{red}(X^{\bullet+})]$. Among eq 2, $E_{ox}(H^{\bullet})$ was reported as −2.307 V versus Fc in AN,[44] while the $E_{red}(X^{\bullet+})$ (V vs Fc) of 120 $X^{\bullet+}$ in AN were available from the published literature[48−52] and displayed in the third column of Table S1.

Step 3 is the chemical process of X (N-containing compounds) abstracting H^+ to produce XH^+, $X + H^+ \rightarrow XH^+$, and the thermodynamic driving force of step 3 is described by the Gibbs free energy of N-containing compounds abstracting H^+ (PA): $\Delta G_{PA}(X)$. $\Delta G_{PA}(X)$ could be calculated by eq 3 in Table 1 using $pK_a(XH^+)$, $\Delta G_{PA}(X) = -1.37pK_a(XH^+)$. Herein, the pK_a values of 120 XH^+ are predicted using the method developed by Luo and co-workers in 2020.[53] The details of the prediction method are shown in the Supporting Information. To further verify the accuracy of predicted $pK_a(XH^+)$ values, the predicted $pK_a(XH^+)$ and the determined $pK_a(XH^+)_D$ values of 24 XH^+[54] in AN are compared in Table S2, and the differences (ΔpK_a) between predicted $pK_a(XH^+)$ and determined $pK_a(XH^+)_D$ are calculated and shown in the last column of Table S2, $\Delta pK_a = pK_a(XH^+) - pK_a(XH^+)_D$. It is clear that ΔpK_a values range

https://doi.org/10.1021/acsomega.4c04209
ACS Omega 2024, 9, 26708−26718

Scheme 2. Chemical Structures of Nitrogen Centered Radical Cations ($X_1^{\bullet+}$ in the Gray Area, $X_2^{\bullet+}$ in the Light Blue Area, $X_3^{\bullet+}$ in the Light Green Area, and $X_4^{\bullet+}$ in the Light Yellow Area) Investigated in this Work, along with the H-Affinities of $X^{\bullet+}$ in Red (kcal/mol), Reduction Potentials of $X^{\bullet+}$ in Blue (V vs Fc), and pK_a of XH^+ in Purple in Acetonitrile (AN)

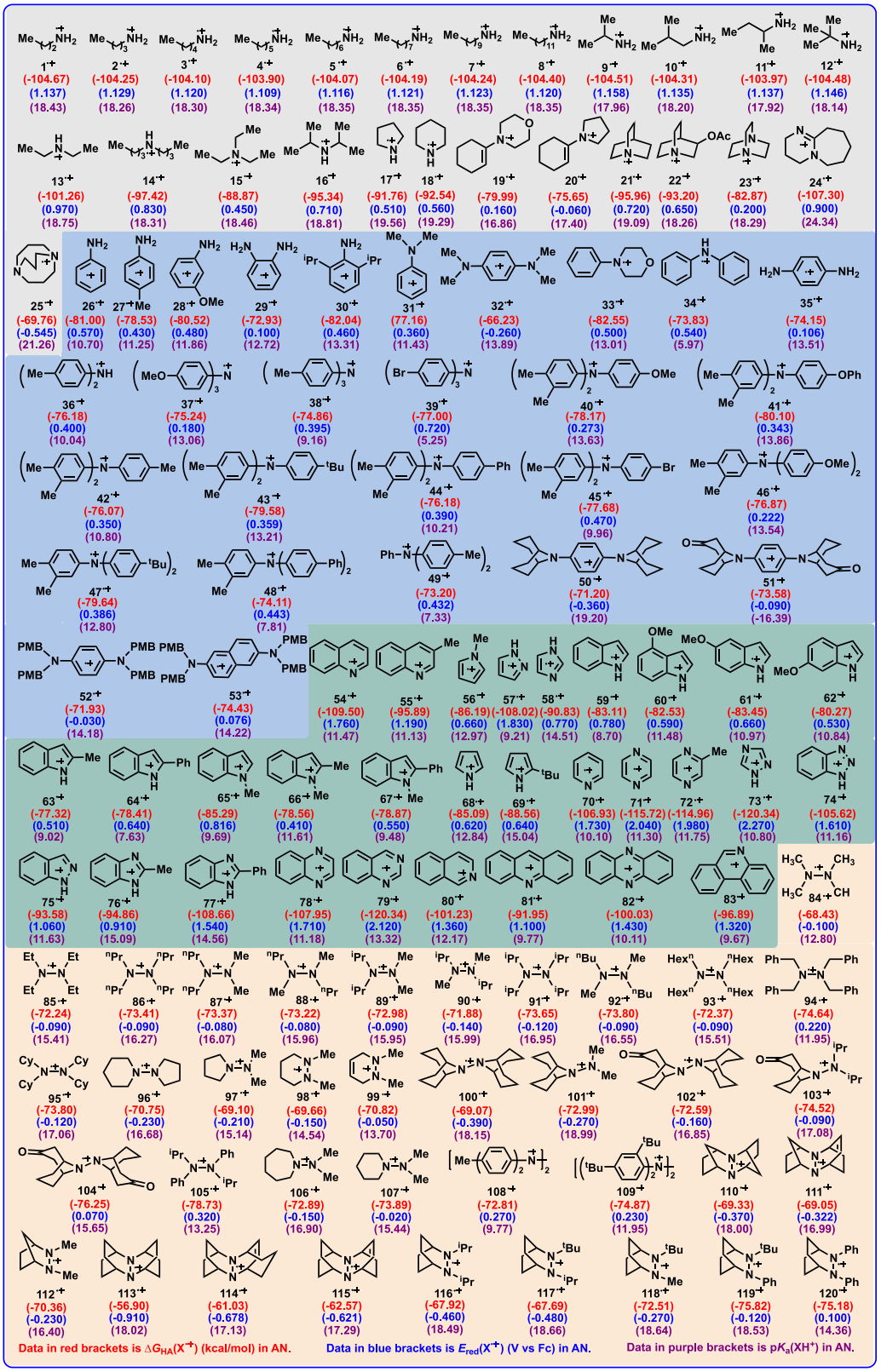

from −0.97 to 0.54, which indicates that the absolute error for the pK_a(XH^+) prediction of 120 XH^+ is estimated within ±1.0 pK_a. All of the pK_a(XH^+) values of 120 XH^+ in AN are summarized in the fourth column of Table S1.

https://doi.org/10.1021/acsomega.4c04209
ACS Omega 2024, 9, 26708−26718

Scheme 3. Classifications of 120 Nitrogen Centered Radical Cations

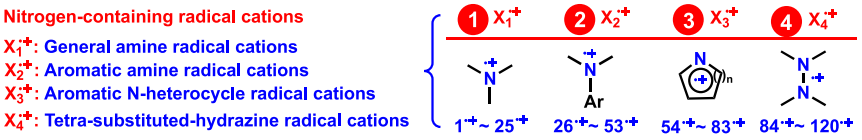

Scheme 4. Thermodynamic Cycle Constructed According to the Chemical Reaction of $X^{\bullet+}$ Abstracting Hydrogen Atoms

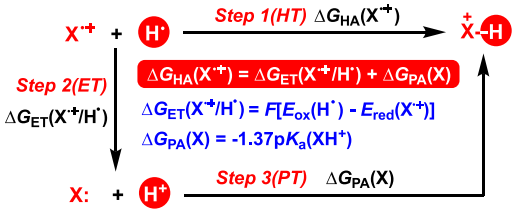

According to the thermodynamic cycle (step 1−step 2−step 3) from Scheme 4, $\Delta G_{HA}(X^{\bullet+})$ values are derived from $\Delta G_{ET}(X^{\bullet+}/H^{\bullet})$ and $\Delta G_{PA}(X)$ by eq 1 of Table 1 using Hess' law,[55,56] $\Delta G_{HA}(X^{\bullet+}) = \Delta G_{ET}(X^{\bullet+}/H^{\bullet}) + \Delta G_{PA}(X)$. The reduction potential experiments are carried out in lab by cyclic voltammetry or Osteryoung square wave voltammetry in AN, and the reproducibility of $E_{red}(X^{\bullet+})$ is ±5 mV.[48−52] Since the absolute error for $pK_a(XH^+)$ prediction of 120 XH^+ is estimated within ±1.0 pK_a, which was verified by the pK_a differences (ΔpK_a) between predicted $pK_a(XH^+)$ and determined $pK_a(XH^+)$ of 24 XH^+ in AN (Table S2), and the reproducibility of determined $E_{red}(X^{\bullet+})$ in AN is ±5 mV, according to the definition of $\Delta G_{HA}(X^{\bullet+})$ in eq 1, the absolute error of $\Delta G_{HA}(X^{\bullet+})$ values is verified as ±1.5 kcal/mol. $\Delta G_{HA}(X^{\bullet+})$ values of 120 $X^{\bullet+}$ in AN are presented in the last column of Table S1. What is more, the $\Delta G_{HA}(X^{\bullet+})$ values, $E_{red}(X^{\bullet+})$ values,[48−52] and $pK_a(XH^+)$ values of 120 $X^{\bullet+}$ in AN are also displayed in Scheme 2.

2.2. $X^{\bullet+}$ Are Potential Alternatives of HAT Catalysts or H-Abstractors. As can be seen from Scheme 2, among 120 $X^{\bullet+}$, **113**$^{\bullet+}$ is thermodynamically the weakest H-abstractor, while **73**$^{\bullet+}$ is thermodynamically the strongest H-abstractor. The H-affinity scale of 120 $X^{\bullet+}$ ranges from −56.90 kcal/mol for **113**$^{\bullet+}$ to −120.34 kcal/mol for **73**$^{\bullet+}$, spanning a very large gap of 63.44 kcal/mol, which indicates that all of the 120 $X^{\bullet+}$ cover from the thermodynamically weak HAT abstractors to thermodynamically very strong HAT abstractors. To reveal the underlying relationship between structures and thermodynamic properties, the H-affinity ranges of $X_1^{\bullet+}$−$X_4^{\bullet+}$ and the H-affinities of some characteristic nitrogen centered radical cations ($X^{\bullet+}$) in AN are summarized in Scheme 5. To quantitatively evaluate the thermodynamic properties of nitrogen centered radical cations investigated in this work, the H-affinities of some common HAT catalysts or reagents in AN are also collected in Scheme 5 for better comparison.

Since $Et_3N^{\bullet+}$ (**15**$^{\bullet+}$, −88.87 kcal/mol),[33−35] ABCO$^{\bullet+}$ (**21**$^{\bullet+}$, −95.96 kcal/mol),[27−32] DABCO$^{\bullet+}$ (**23**$^{\bullet+}$, −82.87 kcal/mol),[36−39] $PhNH_2^{\bullet+}$ (**26**$^{\bullet+}$, −81.00 kcal/mol),[40] Py$^{\bullet+}$ (**70**$^{\bullet+}$, −106.93 kcal/mol),[42,43] TEMPO$^{\bullet}$ (−66.5 kcal/mol),[57,58] PhS$^{\bullet}$ (−78.3 kcal/mol),[51] PINO$^{\bullet}$ (−84.8 kcal/mol),[57,58] and ^{t}BuO$^{\bullet}$ (−104.4 kcal/mol)[59] are frequently used HAT catalyst or reagents in Y−H bond functionalization, it is reasonable to make following judgment criteria. As indicated from the bottom of Scheme 5, (1) if the H-affinity of an $X^{\bullet+}$ is smaller than −60.0 kcal/mol [−60.0 kcal/mol < $\Delta G_{HA}(X^{\bullet+})$], the $X^{\bullet+}$ belongs to a thermodynamically very weak HAT catalyst or H-abstractor. (2) If the H-affinity of an $X^{\bullet+}$ is greater than or equal to −60.0 kcal/mol and smaller than −80.0 kcal/mol [−60.0 kcal/mol ≤ $\Delta G_{HA}(X^{\bullet+})$ < −80.0 kcal/mol], the $X^{\bullet+}$ belongs to a thermodynamically medium-strong HAT catalyst or H-abstractor. (3) If the H-affinity of an $X^{\bullet+}$ is greater than or equal to −80.0 kcal/mol and smaller than −105.0 kcal/mol [−80.0 kcal/mol ≤ $\Delta G_{HA}(X^{\bullet+})$ < −105.0 kcal/mol], the $X^{\bullet+}$ is recognized as a thermodynamically strong HAT catalyst or H-abstractor. (4) If the H-affinity of an $X^{\bullet+}$ is greater than or equal to −105.0 kcal/mol [$\Delta G_{HA}(X^{\bullet+})$ ≤ −105.0 kcal/mol], the $X^{\bullet+}$ is recognized as a thermodynamically very strong HAT catalyst or H-abstractor.

According to the above judgment criteria, TEMPO$^{\bullet}$ (−66.5 kcal/mol) and PhS$^{\bullet}$ (−78.3 kcal/mol) are identified as the thermodynamically medium-strong H-abstractors. $Et_3N^{\bullet+}$ (**15**$^{\bullet+}$, −88.87 kcal/mol), ABCO$^{\bullet+}$ (**21**$^{\bullet+}$, −95.96 kcal/mol), DABCO$^{\bullet+}$ (**23**$^{\bullet+}$, −82.87 kcal/mol), $PhNH_2^{\bullet+}$ (**26**$^{\bullet+}$, −81.00 kcal/mol), PINO$^{\bullet}$ (−84.8 kcal/mol), and ^{t}BuO$^{\bullet}$ (−104.4 kcal/mol) are identified as the thermodynamically strong H-abstractors. Py$^{\bullet+}$ (**70**$^{\bullet+}$, −106.93 kcal/mol) belongs to a thermodynamically very strong HAT catalyst or H-abstractor, which is thermodynamically even better H-abstractor than H$^{\bullet}$ (−102.3 kcal/mol)[51] in AN.

Among 120 $X^{\bullet+}$ and except **113**$^{\bullet+}$ (−56.9 kcal/mol), the H-affinity scale ranges from −61.03 kcal/mol for **114**$^{\bullet+}$ to −120.34 kcal/mol for **73**$^{\bullet+}$, which means that $X^{\bullet+}$ generally belongs to thermodynamically medium-strong, strong, or very strong H-abstractors. To be precise, 11 $X^{\bullet+}$ (**24**$^{\bullet+}$, **54**$^{\bullet+}$, **57**$^{\bullet+}$, **70**$^{\bullet+}$−**74**$^{\bullet+}$, and **77**$^{\bullet+}$−**79**$^{\bullet+}$) are recognized as the thermodynamically very strong H-abstractors with $\Delta G_{HA}(X^{\bullet+})$ < −105.0 kcal/mol. 42 $X^{\bullet+}$ (**1**$^{\bullet+}$−**18**$^{\bullet+}$, **21**$^{\bullet+}$−**23**$^{\bullet+}$, **26**$^{\bullet+}$, **28**$^{\bullet+}$, **30**$^{\bullet+}$, **33**$^{\bullet+}$, **41**$^{\bullet+}$, **55**$^{\bullet+}$−**56**$^{\bullet+}$, **58**$^{\bullet+}$−**62**$^{\bullet+}$, **65**$^{\bullet+}$, **68**$^{\bullet+}$−**69**$^{\bullet+}$, **75**$^{\bullet+}$−**76**$^{\bullet+}$, and **80**$^{\bullet+}$−**83**$^{\bullet+}$) are recognized as the thermodynamically strong H-abstractors with −80.0 kcal/mol ≤ $\Delta G_{HA}(X^{\bullet+})$ < −105.0 kcal/mol. 66 $X^{\bullet+}$ (**19**$^{\bullet+}$−**20**$^{\bullet+}$, **25**$^{\bullet+}$, **27**$^{\bullet+}$, **29**$^{\bullet+}$, **31**$^{\bullet+}$−**32**$^{\bullet+}$,

Table 1. Chemical Processes, Thermodynamic Parameters, and Computed Equations of Step 1−Step 3 for $X^{\bullet+}$ Abstracting Hydrogen Atoms to Generate XH^+ in AN

step *X*	chemical process	parameters and computed equations	eq *X*
step 1 (HT)	$X^{\bullet+} + H^{\bullet} \rightarrow XH^+$	$\Delta G_{HA}(X^{\bullet+}) = \Delta G_{ET}(X^{\bullet+}/H^{\bullet}) + \Delta G_{PA}(X)$ (1)	1
step 2 (ET)	$X^{\bullet+} + H^{\bullet} \rightarrow X: + H^+$	$\Delta G_{ET}(X^{\bullet+}/H^{\bullet}) = F[E_{ox}(H^{\bullet}) - E_{red}(X^{\bullet+})]$ (2)	2
step 3 (PT)	$X + H^+ \rightarrow XH^+$	$\Delta G_{PA}(X) = -1.37pK_a(XH^+)$ (3)	3

https://doi.org/10.1021/acsomega.4c04209
ACS Omega 2024, 9, 26708−26718

Scheme 5. Thermodynamic Comparisons on H-Affinities of $X_1^{\bullet+}$–$X_4^{\bullet+}$ and Common Radicals ($Y^{\bullet}$), along with H-Affinities of Some Characteristic $X^{\bullet+}$ in AN (kcal/mol)

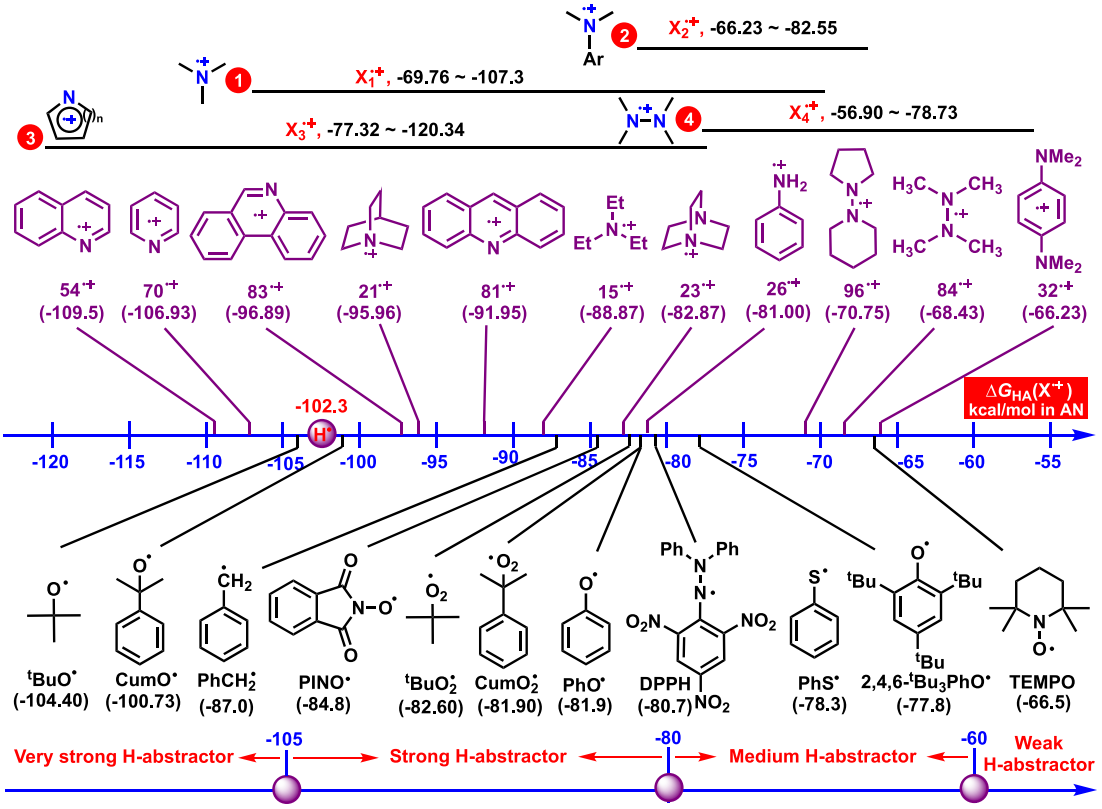

34$^{\bullet+}$–**40**$^{\bullet+}$, **42**$^{\bullet+}$–**53**$^{\bullet+}$, **63**$^{\bullet+}$–**64**$^{\bullet+}$, **66**$^{\bullet+}$–**67**$^{\bullet+}$, **84**$^{\bullet+}$–**112**$^{\bullet+}$, and **114**$^{\bullet+}$–**120**$^{\bullet+}$) are recognized as the thermodynamically medium-strong H-abstractors with −60.0 kcal/mol ≤ $\Delta G_{HA}(X^{\bullet+})$ < −80.0 kcal/mol. Only **113**$^{\bullet+}$ (−56.90 kcal/mol) belongs to the thermodynamically weak H-abstractor. That is, most $X^{\bullet+}$ (108 = 66 + 42) are thermodynamically medium-strong or strong H-abstractors.

From Scheme 5, it is obvious that the H-affinity scale ranges from −69.76 kcal/mol (**25**$^{\bullet+}$) to −107.30 kcal/mol (DBU$^{\bullet+}$) for $X_1^{\bullet+}$, from −66.23 kcal/mol (**32**$^{\bullet+}$) to −82.55 kcal/mol (**33**$^{\bullet+}$) for $X_2^{\bullet+}$, from −77.32 kcal/mol (**63**$^{\bullet+}$) to −120.34 kcal/mol (**73**$^{\bullet+}$) for $X_3^{\bullet+}$, and from −61.03 kcal/mol (**114**$^{\bullet+}$) to −78.73 kcal/mol (**105**$^{\bullet+}$) for $X_4^{\bullet+}$ except **113**$^{\bullet+}$ (−56.90 kcal/mol). Normally, the H-affinities have the following regular pattern: $X_2^{\bullet+} \approx X_4^{\bullet+} < X_1^{\bullet+} \approx X_3^{\bullet+}$, implying that $X_2^{\bullet+}$ and $X_4^{\bullet+}$ have similar thermodynamic H-abstraction properties, while $X_1^{\bullet+}$ and $X_3^{\bullet+}$ have the similar thermodynamic H-abstraction properties. In light of H-affinity scales, $X_1^{\bullet+}$ (−69.76 to −107.30 kcal/mol) with the structure of general amine radical cations and $X_3^{\bullet+}$ (−77.73 to −120.34 kcal/mol) with the structure of aromatic N-heterocycle radical cations generally belong to the thermodynamically medium-strong, strong, or very strong H-abstractors. $X_2^{\bullet+}$ (−66.23 to 82.55 kcal/mol) with the structure of aromatic amine radical cations and $X_4^{\bullet+}$ (−61.03 to −78.73 kcal/mol except **113**$^{\bullet+}$) with the structure of tetrasubstituted-hydrazine radical cations generally belong to the thermodynamically medium-strong H-abstractors.

Since $Et_3N^{\bullet+}$ (**15**$^{\bullet+}$, −88.87 kcal/mol),[33−35] ABCO$^{\bullet+}$ (**21**$^{\bullet+}$, −95.96 kcal/mol),[27−32] DABCO$^{\bullet+}$ (**23**$^{\bullet+}$, −82.87 kcal/mol),[36−39] and Py$^{\bullet+}$ (**70**$^{\bullet+}$, −106.93 kcal/mol)[42,43] have been widely applied into Y–H bond functionalization via HAT strategy, according to their H-affinities data, it is reasonable to infer that $X_1^{\bullet+}$ with the structure of general amine radical cations and $X_3^{\bullet+}$ with the structure of aromatic N-heterocycle radical cations are a type of potential HAT catalysts in Y–H bond functionalization, which should be paid more attention by synthetic chemists.

Additionally, several valuable conclusions can be made as follows.

(1) As for general amine radical cations $X_1^{\bullet+}$, the H-affinities are strongly affected by the number of substituents in central nitrogen-atom. Specifically, the H-affinities of monosubstituted amine radical cations (**1**$^{\bullet+}$–**12**$^{\bullet+}$) range from −103.90 kcal/mol (**4**$^{\bullet+}$) to −104.67 kcal/mol (**1**$^{\bullet+}$), which indicates that monosubstituted amine radical cations (**1**$^{\bullet+}$–**12**$^{\bullet+}$) are the thermodynamically strong H-abstractors with $\Delta G_{HA}(X^{\bullet+})$ < −100.0 kcal/mol. The H-affinities of disubstituted amine radical cations (**13**$^{\bullet+}$–**18**$^{\bullet+}$) range from −88.87 kcal/mol (**15**$^{\bullet+}$) to −101.26 kcal/mol (**13**$^{\bullet+}$), which means that disubstituted amine radical cations (**13**$^{\bullet+}$–**18**$^{\bullet+}$) are the thermodynamically strong H-abstractors with $\Delta G_{HA}(X^{\bullet+})$ < −88.0 kcal/mol. The H-affinities of trisubstituted amine radical cations (**19**$^{\bullet+}$–**25**$^{\bullet+}$) range from −69.76 kcal/mol (**25**$^{\bullet+}$) to −107.30 kcal/mol (DBU$^{\bullet+}$ or **24**$^{\bullet+}$), which indicates that H-affinities of trisubstituted amine radical cations (**19**$^{\bullet+}$–**25**$^{\bullet+}$) span a wide range of 37.54 kcal/mol, and cover from thermodynamically medium-strong to very strong H-abstractors due to their various trisubstituted structures.

(2) Most aromatic amine radical cations $X_2^{\bullet+}$ are medium-strong H-abstractors. Since H-affinities of $X_2^{\bullet+}$ (**26**$^{\bullet+}$–

https://doi.org/10.1021/acsomega.4c04209
ACS Omega 2024, 9, 26708−26718

Scheme 6. Thermodynamic Comparisons on H-Affinities of $X_1^{\bullet+}$−$X_4^{\bullet+}$ and Frequently Used Oxidative MS-PCET Reagents in AN (kcal/mol)

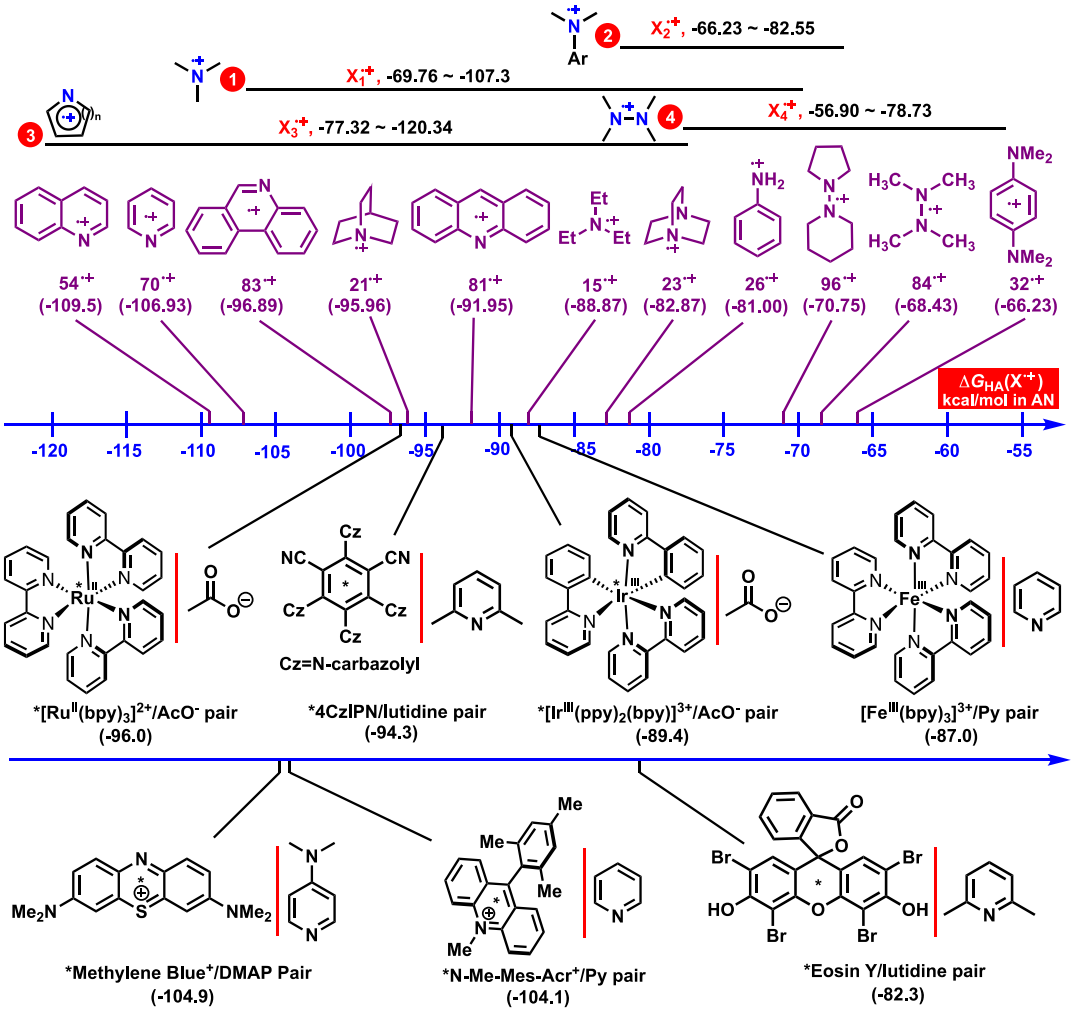

$53^{\bullet+}$) range from −66.23 kcal/mol to −82.55 kcal/mol; therefore, the thermodynamic H-abstraction abilities of $X_2^{\bullet+}$ are between TEMPO$^{\bullet}$ (−66.5 kcal/mol)[51] and PINO$^{\bullet}$ (−84.8 kcal/mol).[51] Most H-affinities of $X_2^{\bullet+}$ are smaller than −80.0 kcal/mol [$\Delta G_{HA}(X_2^{\bullet+}) > -80.0$ kcal/mol, $27^{\bullet+}$, $29^{\bullet+}$, $31^{\bullet+}$, $32^{\bullet+}$, and $34^{\bullet+}$−$53^{\bullet+}$); therefore, most aromatic amine radical cations $X_2^{\bullet+}$ are medium-strong H-abstractors.

(3) Aromatic N-heterocycle radical cations $X_3^{\bullet+}$ with various structures have significant differences in thermodynamic H-abstraction abilities, and not all $X_3^{\bullet+}$ are thermodynamically strong or very strong H-abstractors. The H-affinities of $X_3^{\bullet+}$ (−77.32 to −120.34 kcal/mol) suggest that not all aromatic N-heterocycle radical cations are thermodynamically strong [−80.0 kcal/mol ≤ $\Delta G_{HA}(X^{\bullet+})$ < −105.0 kcal/mol] or very strong [$\Delta G_{HA}(X^{\bullet+}) \leq -105.0$ kcal/mol] H-abstractors. $X_3^{\bullet+}$ with various structures have significant differences in thermodynamic H-abstraction abilities, such as the H-affinities of $63^{\bullet+}$ (−77.32 kcal/mol) and $73^{\bullet+}$ (−120.43 kcal/mol). Furthermore, the thermodynamic H-abstraction abilities could be regulated by adjusting different substituents in aromatic N-heterocycles, such as $59^{\bullet+}$−$67^{\bullet+}$ (−77.32 to −85.29 kcal/mol) owning the same parent structure of indole.

(4) Tetra-substituted-hydrazine radical cations $X_4^{\bullet+}$ (−56.9 to −78.3 kcal/mol for $84^{\bullet+}$−$120^{\bullet+}$) are unsuitable to be applied as H-abstractors in Y−H bond functionalization, in contrast, the X_4H^+ can act as good H-donors in chemical reactions to quench key radicals generating the desired products.

Since nitrogen centered radical cations ($X^{\bullet+}$) are highly unstable intermediates in solution, $X^{\bullet+}$ may undergo deprotonation from α−C−H bonds (if have) or other degradation.[24−26,35] According to the definition for H-affinities of $X^{\bullet+}$, the thermodynamic potential of $X^{\bullet+}$ abstracting hydrogen atoms is dependent on the reduction potentials of $X^{\bullet+}$ and the pK_a of XH^+; therefore, the deprotonation and degradation processes of $X^{\bullet+}$ do not affect the thermodynamic evaluation on H-affinities of $X^{\bullet+}$ as a type of HAT reagents or catalysts. In addition, whether $X^{\bullet+}$ acts as a hydrogen atom abstractor, proton donor, or hydrogen atom donor relies on the existing reaction conditions. For example, the $Et_3N^{\bullet+}$ ($15^{\bullet+}$) was designed to function as hydrogen atom abstractors,[33] proton donors,[25,26,35] or hydrogen atom donors[24,35] in chemical transformations, respectively.

2.3. $X^{\bullet+}$ Are Potential Alternatives of Oxidative MS-PCET Reagents in Chemical Reactions. MS-PCET strategy has been broadly researched and successfully employed in organic synthesis,[17−23] in which a proton and an electron from

https://doi.org/10.1021/acsomega.4c04209
ACS Omega 2024, 9, 26708−26718

Scheme 7. Thermodynamic Comparisons of *Ir^{III}/ABCO Pair Acting as HAT and MS-PCET Reagent, Respectively, in AN

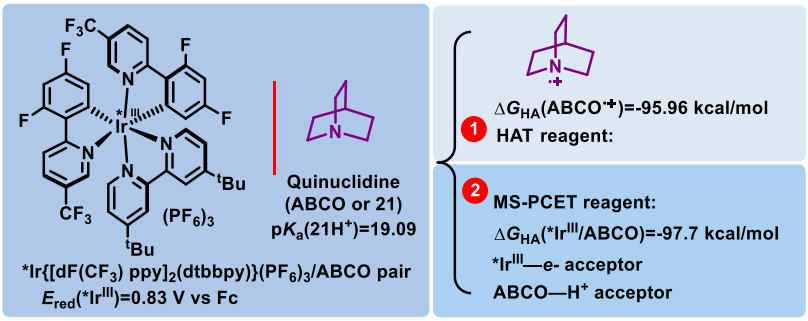

or to different sites transfer in a concerted elementary step. For oxidative MS-PCET,[17] a single-electron oxidant/Brønsted base pair (Ox^+/B^- pair) can act as a formal hydrogen atom ($H^•$) abstractor, in which an electron transfers to single-electron oxidant, while a proton transfers to the Brønsted base. The combination of a strong single-electron oxidant and a strong Brønsted base could overcome the high energy barrier of Y−H bond dissociation and activate the strong Y−H bond into $Y^•$.[17] The stronger the oxidation potential of a single-electron oxidant is, and the stronger the basicity of Brønsted base is, the stronger the H-affinity of the Ox^+/B^- pair is.[17] Due to the very high single-electron oxidation ability of the photocatalyst; therefore, the photoexcited catalyst/Brønsted base pair ($*PC^+/B^-$ pair) is a type of efficient and significant oxidative MS-PCET reagent in chemical synthesis.[17] Since both $X^{•+}$ and oxidative MS-PCET reagents are efficient H-abstractors in chemical reactions and they both need single-electron oxidant/Brønsted base pair to achieve the activated function,[17] it is necessary to compare the thermodynamic H-abstraction abilities between $X^{•+}$ and oxidative MS-PCET reagents to clarify their thermodynamic differences.

Herein, the H-affinities of frequently used oxidative MS-PCET reagents,[17,60,61] such as $*[Ru^{II}(bpy)_3]^{2+}/AcO^-$ pair (−96.0 kcal/mol),[17] $*[Ir^{III}(ppy)_2(bpy)]^{3+}/AcO^-$ pair (−89.4 kcal/mol),[17] $[Fe^{III}(bpy)_3]^{3+}$/Py pair (−87.0 kcal/mol),[17] *4CzIPN/lutidine pair (94.3 kcal/mol),[17] *methylene $blue^+$/DMAP pair (−104.9 kcal/mol),[17] *N-Me-Mes-Acr^+/Py pair (−104.1 kcal/mol),[17] and *eosin Y/lutidine pair (−82.3 kcal/mol),[17] in AN are collected in Scheme 6, along with the H-affinities of $X^{•+}$ ($X_1^{•+}$−$X_4^{•+}$). From Scheme 6, it is clear that the H-affinities of these seven oxidative MS-PCET reagents range from −82.3 kcal/mol (*eosin Y/lutidine pair) to −104.9 kcal/mol (*methylene $blue^+$/DMAP pair), which all belong to medium-strong or strong hydrogen atom abstractors.

According to the H-affinities scales, it is found that $X_2^{•+}$ (−66.23 to −82.55 kcal/mol) and $X_4^{•+}$ (−56.9 to 78.73 kcal/mol) are generally weak H-abstractors than oxidative MS-PCET reagents, demonstrating that $X_2^{•+}$ and $X_4^{•+}$ are not ideal alternatives of oxidative MS-PCET reagents in chemical reactions. About 11 $X^{•+}$ from $X_1^{•+}$ and $X_3^{•+}$ (**24**$^{•+}$, **54**$^{•+}$, **57**$^{•+}$, **70**$^{•+}$−**74**$^{•+}$, and **77**$^{•+}$−**79**$^{•+}$) are thermodynamically even better H-abstractors than the *methylene $blue^+$/DMAP pair (−104.9 kcal/mol) and *N-Me-Mes-Acr^+/Py pair (−104.1 kcal/mol) in AN. About 42 $X^{•+}$ from $X_1^{•+}$ and $X_3^{•+}$ (**1**$^{•+}$−**18**$^{•+}$, **21**$^{•+}$−**23**$^{•+}$, **26**$^{•+}$, **28**$^{•+}$, **30**$^{•+}$, **33**$^{•+}$, **41**$^{•+}$, **55**$^{•+}$−**56**$^{•+}$, **58**$^{•+}$−**62**$^{•+}$, **65**$^{•+}$, **68**$^{•+}$−**69**$^{•+}$, **75**$^{•+}$−**76**$^{•+}$, and **80**$^{•+}$−**83**$^{•+}$) are the thermodynamic alternatives of oxidative MS-PCET reagents in chemical reactions, whose H-affinities are greater than −80.0 kcal/mol and smaller than −105.0 kcal/mol in AN. These thermodynamic results suggest us to pay more attention to the H-abstraction properties of general amine radical cations and aromatic N-heterocycle radical cations, and they are a type of important HAT catalysts or H-abstractors.

It should be pointed out that the N-containing compound (X) must be activated by a single-electron oxidant, especially a photoexcited photocatalyst, into $X^{•+}$ first (Scheme 1),[27−43] accordingly, a single-electron oxidant/N-containing compound pair (Ox^+/X pair) must be constructed to generate $X^{•+}$ species in HAT reactions.[17] Since the N-containing compound (X) is one type of organic Brønsted base, outwardly, it seems to be the same that a single-electron oxidant/Brønsted base pair is involved in both HAT reactions and MS-PCET reactions.[17] Although both HAT reactions and MS-PCET reactions need a single-electron oxidant/Brønsted base pair, the roles of N-containing compound (X) in HAT reactions and MS-PCET reactions are totally different. In HAT reactions, N-containing compounds (X) should be transformed into nitrogen centered radical cations ($X^{•+}$), which are the real HAT catalysts or H-abstractors.[27−43] However, in MS-PCET reactions, N-containing compounds (X) just act as the proton abstractors.[17−23]

Besides the different roles of N-containing compounds (X) in the single-electron oxidant/X pair, the thermodynamic H-abstraction abilities of a single-electron oxidant/X pair in HAT reactions and MS-PCET reactions are also different. Herein, *Ir{[$dF(CF_3)ppy]_2(dtbbpy)$}$(PF_6)_3$/ABCO pair (*Ir^{III}/ABCO pair) is selected as an example to elucidate the thermodynamic differences between them (Scheme 7). When the *Ir^{III}/ABCO pair acts as the HAT reagent, ABCO (E_{ox} = 0.720 V vs Fc) is oxidated into ABCO$^{•+}$ by the photocatalyst *Ir^{III} [E_{red}(*Ir^{III}) = 0.83 V vs Fc in AN].[17] ABCO$^{•+}$ is the real H-abstractor or catalyst in chemical reactions, and the H-affinity of ABCO$^{•+}$ is estimated as −95.96 kcal/mol in AN. However, when the *Ir^{III}/ABCO pair acts as an MS-PCET reagent, the H-affinity of the *Ir^{III}/ABCO pair is dependent on the reduction potential of *Ir^{III} [E_{red}(*Ir^{III}) = 0.83 V vs Fc] and the pK_a of $ABCOH^+$ (19.09 calculated in MeCN), $\Delta G_{HA}(*Ir^{III}/ABCO) = F[E_{red}(*Ir^{III}) + E_{ox}(H^•)] + 1.37pK_a(ABCOH^+)$, which is estimated as −97.7 kcal/mol in AN. If the H-affinity of ABCO$^{•+}$ is compared with that of the *Ir^{III}/ABCO pair, it can be discovered that the difference of thermodynamic H-abstraction abilities for ABCO$^{•+}$ (−95.96 kcal/mol) and the *Ir^{III}/ABCO pair (−97.70 kcal/mol) is not significant, and they both belong to the thermodynamically strong H-abstractors.

Therefore, it raises another important question: when does the *Ir^{III}/ABCO pair function as a HAT reagent or a MS-PCET reagent? it can be assumed that the type of substrate to be activated determines the H-abstraction mechanism. If the

https://doi.org/10.1021/acsomega.4c04209
ACS Omega 2024, 9, 26708−26718

Scheme 8. Thermodynamic Comparisons between H-Affinities of $X_1^{\bullet+}$–$X_4^{\bullet+}$ and BDFE of Various Representative Y–H Bonds (Homolytic Energy) in AN (kcal/mol)

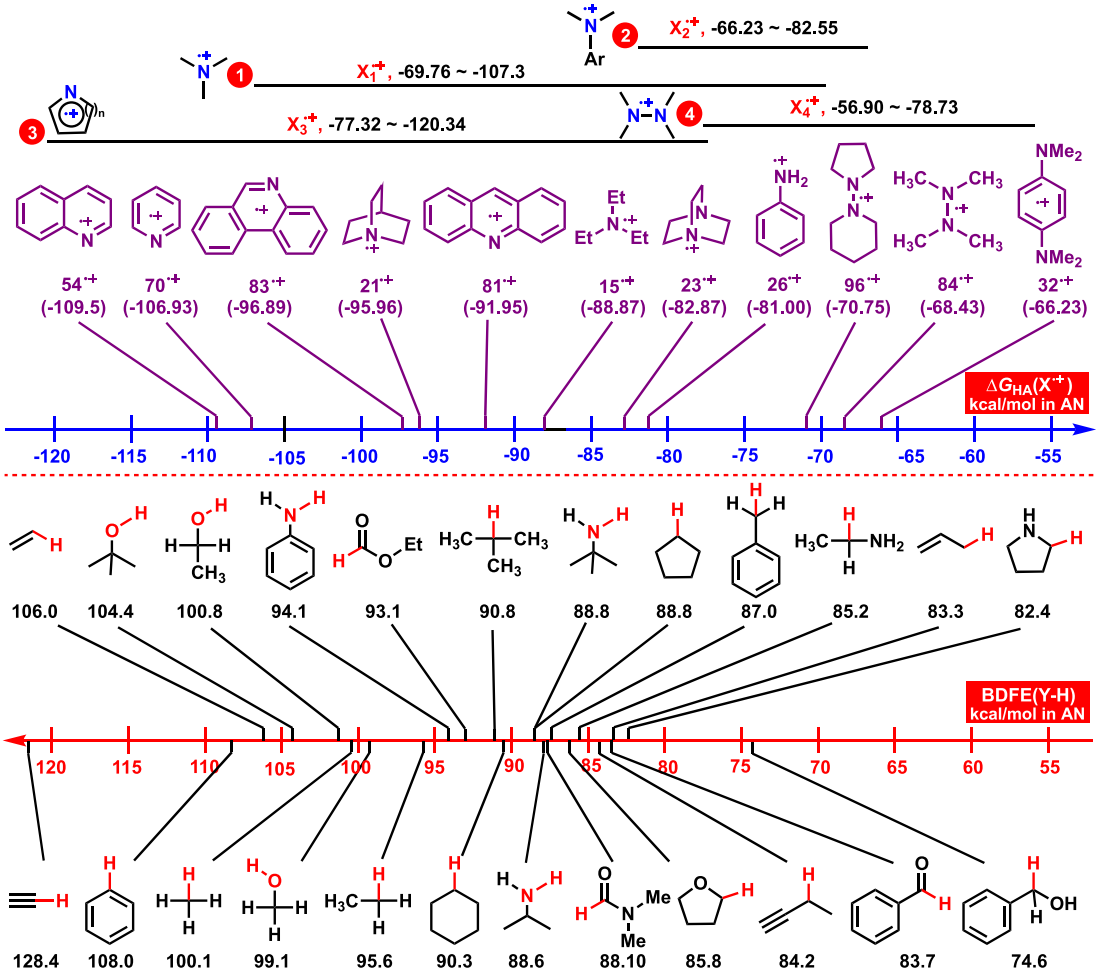

substrate is a weak polar Y–H bond, direct HAT from Y–H bond to $X^{\bullet+}$ may be favorable.[27−32] In addition, if the substrate is a strong polar Y–H bond, perhaps the MS-PCET mechanism of hydrogen atom transferring from Y–H bond to $*Ir^{III}$ and ABCO, respectively, may be favorable.[17−23] The thermodynamic H-abstraction properties of the $X^{\bullet+}$ and $*Ir^{III}$/ABCO pairs acting as HAT or MS-PCET reagents remind us to probe far into the H-abstraction process and find more mechanistic evidence.

2.4. Applications of $X^{\bullet+}$ into Y–H Bond Functionalization as a Type of Potential H-Abstraction Reagents. According to the thermodynamic results of H-affinity for $X^{\bullet+}$, nitrogen centered radical cations are definitely potential H-abstractors in Y–H bond functionalization. For a Y–H bond, the bond dissociation free energy (BDFE) of the Y–H bond, BDFE(Y–H), is a very important thermodynamic parameter to evaluate the bond strength and breaking difficulty.[62−65] Based on the H-affinities of $X^{\bullet+}$ and the BDFE(Y–H) values, the thermodynamic driving forces of HAT from the Y–H bond to $X^{\bullet+}$ ($X^{\bullet+}$ + Y–H → XH^+ + $Y^{\bullet}$) could be calculated by subsequent eq 4

$$\Delta G_{HAT}(X^{\bullet}/YH) = \Delta G_{HA}(X^{\bullet+}) + BDEF(YH)) \quad (4)$$

If the $\Delta G_{HAT}(X^{\bullet+}/YH)$ value is greater than 0, $\Delta G_{HAT}(X^{\bullet+}/YH) > 0$, the H-abstraction process from YH to $X^{\bullet+}$ is thermodynamically unfavorable. If the $\Delta G_{HAT}(X^{\bullet+}/YH)$ value is more negative than 0, $\Delta G_{HAT}(X^{\bullet+}/YH) < 0$, the H-abstraction process from YH to $X^{\bullet+}$ is thermodynamically feasible.

Herein, the BDFE of various representative Y–H bonds,[62−65] consisting of C_{sp^3}–H, C_{sp^2}–H, C_{sp}–H, N–H, and O–H bonds, in AN are gathered and displayed in Scheme 8, along with the H-affinities of $X^{\bullet+}$ ($X_1^{\bullet+}$–$X_4^{\bullet+}$). As shown in Scheme 8, it can be discovered that BDFE(Y–H) ranges from 74.6 kcal/mol for C_{sp^3}–H bond in benzylalcohol (α-HO-C_{sp^3}–H) to 128.4 kcal/mol for C_{sp}–H bond in CH≡CH among the 24 Y–H bonds, covering a very large thermodynamic scale by 53.8 kcal/mol.

Several interesting conclusions could be drawn according to the thermodynamic results: (1) C_{sp}–H bond (BDFE = 128.4 kcal/mol) in the CH≡CH molecule is the most difficult to be activated by the direct HAT process among the 24 Y–H bonds, and pyrrodiazole radical cation [$73^{\bullet+}$, $\Delta G_{HA}(73^{\bullet+})$ = −120.34 kcal/mol] is the strongest H-abstractor among 120 $X^{\bullet+}$ investigated in this work. However, $73^{\bullet+}$ could not activate C_{sp}–H via HAT from the view of thermodynamics. (2) $X_2^{\bullet+}$ [$\Delta G_{HA}(X_2^{\bullet+})$ = −66.73 to −82.55 kcal/mol] and $X_4^{\bullet+}$ [$\Delta G_{HA}(X_4^{\bullet+})$ = −56.90 to −78.73 kcal/mol] would not be the first choice to activate a variety of Y–H bonds [BDFE(Y–H) = 74.6 − 128.4 kcal/mol], and few of them have the thermodynamic capability to abstract hydrogen atoms from the Y–H bond. (3) $X_1^{\bullet+}$ [$\Delta G_{HA}(X_1^{\bullet+})$ = −75.65 to −104.67 kcal/

https://doi.org/10.1021/acsomega.4c04209
ACS Omega 2024, 9, 26708−26718

mol except $25^{\bullet+}$] and $X_3^{\bullet+}$ [$\Delta G_{HA}(X_3^{\bullet+})$ = −77.32 to −120.34 kcal/mol] could establish a practical library of H-abstractors owning various thermodynamic properties to activate various Y−H bonds [BDFE(Y−H) = 74.6−128.4 kcal/mol]. (4) The combination of Schemes 2 and 8 is a significant instructional tool to help synthetic chemists choose suitable H-abstractors to activate and functionalize various Y−H bonds. For example, $ABCO^{\bullet+}$ ($\mathbf{21}^{\bullet+}$, −95.96 kcal/mol) could be selected to activate N−H bond from alkylamine, C_{sp^2}−H bond from aldehyde and amide, as well as α-C_{sp^3}−H bonds from amine, alkyne, alkenyl group, alcohol, aryl group, and ether group, but $ABCO^{\bullet+}$ could not be used to activate C_{sp^2}−H, C_{sp}−H, O−H, and C_{sp^3}−H of the methyl group from alkane.

3. CONCLUSIONS

In summary, as a type of HAT catalyst or H-abstractor, the H-affinity of $X^{\bullet+}$ is a significant thermodynamic parameter to quantitatively measure the thermodynamic H-abstraction reactivity of an $X^{\bullet+}$, and provide valuable guidelines for the application of $X^{\bullet+}$ in the Y−H bond functionalization. In this work, the pK_a values of 120 XH^+ in AN are predicted, and the H-affinities of 120 $X^{\bullet+}$ are derived from the $E_{red}(X^{\bullet+})$ and p$K_a(XH^+)$ using Hess' law by constructing a thermodynamic cycle. The thermodynamic H-abstraction properties of 120 $X^{\bullet+}$ in AN have been discussed in detail, and several worthy conclusions can be drawn as follows: (1) $X^{\bullet+}$ are potential alternatives of HAT catalysts or H-abstractors. (2) The thermodynamic H-abstraction properties of $X_1^{\bullet+}$−$X_4^{\bullet+}$ are closely related to their chemical structures. (3) $X^{\bullet+}$ are potential alternatives of oxidative MS-PCET reagents in chemical reactions. (4) Roles of N-containing compound (X) are totally different in a single-electron oxidant/X pair in HAT and MS-PCET reactions, and the thermodynamic H-abstraction abilities are also different. (5) A combination of Schemes 2 and 8 is a significant instructional tool to help synthetic chemists choose suitable H-abstractors to activate and functionalize various Y−H bonds.

4. METHODS

The pK_a values of 120 XH^+ in AN were predicted by the method developed by Luo and co-workers in 2020 at http://pka.luoszgroup.com/prediction. Prediction methods: XGBoost with RMSE = 1.79 and r^2 = 0.918 (80:20 train test split). The accuracy of the predicted p$K_a(XH^+)$ in AN is verified as ±1.0 pK_a in this work (Table S2).

■ ASSOCIATED CONTENT

Supporting Information

The Supporting Information is available free of charge at https://pubs.acs.org/doi/10.1021/acsomega.4c04209.

Original data of pK_a prediction of 120 XH^+ (PDF)

■ AUTHOR INFORMATION

Corresponding Authors

Bao-Chen Qian − *College of Medical Engineering, Jining Medical University, Jining, Shandong 272000, P. R. China*; Email: qianbc@mail.jnmc.edu.cn

Guang-Bin Shen − *College of Medical Engineering, Jining Medical University, Jining, Shandong 272000, P. R. China*; orcid.org/0000-0003-0449-7301; Email: gbshen@mail.jnmc.edu.cn

Authors

Xia Zhao − *College of Medical Engineering, Jining Medical University, Jining, Shandong 272000, P. R. China*

Yi-Lin Hou − *College of Medical Engineering, Jining Medical University, Jining, Shandong 272000, P. R. China*

Complete contact information is available at: https://pubs.acs.org/10.1021/acsomega.4c04209

Notes

The authors declare no competing financial interest.

■ ACKNOWLEDGMENTS

We acknowledge support for this work from the Natural Science Foundation of Shandong Province (grant no. ZR2022QB201), Health Commission of Shandong Province (202313051336), and Jining Medical University (startup grant nos. 600945001 and 600841002).

■ REFERENCES

(1) Chan, A. Y.; Perry, I. B.; Bissonnette, N. B.; Buksh, B. F.; Edwards, G. A.; Frye, L. I.; Garry, O. L.; Lavagnino, M. N.; Li, B. X.; Liang, Y.; Mao, E.; Millet, A.; Oakley, J. V.; Reed, N. L.; Sakai, H. A.; Seath, C. P.; MacMillan, D. W. C. Metallaphotoredox: The Merger of Photoredox and Transition Metal Catalysis. *Chem. Rev.* **2022**, *122*, 1485−1542.

(2) Zhang, J.; Rueping, M. Metallaphotoredox Catalysis for sp^3 C-H Functionalizations through Hydrogen Atom Transfer (HAT). *Chem. Soc. Rev.* **2023**, *52*, 4099−4120.

(3) Jiang, T.; Liu, H.; Zhang, H.; Huang, H. Catalytic Benzylation Reactions: From C-H Bond Activation to C-N Bond Activation. *Chin. J. Chem.* **2021**, *39*, 1070−1078.

(4) Wiesenfeldt, M. P.; Rossi-Ashton, J. A.; Perry, I. B.; Diesel, J.; Garry, O. L.; Bartels, F.; Coote, S. C.; Ma, X.; Yeung, C. S.; Bennett, D. J.; MacMillan, D. W. C. General Access to Cubanes as Benzene Bioisosteres. *Nature* **2023**, *618*, 513−518.

(5) Brandes, D. S.; Ellman, J. A. C-H Bond Activation and Sequential Addition to Two Different Coupling Partners: A Versatile Approach to Molecular Complexity. *Chem. Soc. Rev.* **2022**, *51*, 6738−6756.

(6) Sinha, S. K.; Guin, S.; Maiti, S.; Biswas, J. P.; Porey, S.; Maiti, D. Toolbox for Distal C-H Bond Functionalizations in Organic Molecules. *Chem. Rev.* **2022**, *122*, 5682−5841.

(7) Bisht, R.; Haldar, C.; Hassan, M. M. M.; Hoque, M. E.; Chaturvedi, J.; Chattopadhyay, B. Metal-catalysed C−H bond activation and borylation. *Chem. Soc. Rev.* **2022**, *51*, 5042−5100.

(8) Zhang, Z.; Chen, P.; Liu, G. Copper-Catalyzed Radical Relay in C(sp^3)-H Functionalization. *Chem. Soc. Rev.* **2022**, *51*, 1640−1658.

(9) Xiang, H.; Ye, Y. Cu-Catalyzed α-Alkylation of Glycine Derivatives for C(sp^3)-H/C(sp^3)-H Bond Selective Functionalization. *ACS Catal.* **2024**, *14*, 522−532.

(10) Capaldo, L.; Ravelli, D.; Fagnoni, M. Direct Photocatalyzed Hydrogen Atom Transfer (HAT) for Aliphatic C−H Bonds Elaboration. *Chem. Rev.* **2022**, *122*, 1875−1924.

(11) Galeotti, M.; Salamone, M.; Bietti, M. Electronic Control over Site-Selectivity in Hydrogen Atom Transfer (HAT) Based C(Sp^3)-H Functionalization Promoted by Electrophilic Reagents. *Chem. Soc. Rev.* **2022**, *51*, 2171−2223.

(12) Selected reviews (a) Chang, L.; Wang, S.; An, Q.; Liu, L.; Wang, H.; Li, Y.; Feng, K.; Zuo, Z. Resurgence and Advancement of Photochemical Hydrogen Atom Transfer Processes in Selective Alkane Functionalizations. *Chem. Sci.* **2023**, *14*, 6841−6859. (b) Zhang, S.; Findlater, M. Electrochemically Driven Hydrogen Atom Transfer Catalysis: A Tool for C(sp^3)/Si-H Functionalization and Hydrofunctionalization of Alkenes. *ACS Catal.* **2023**, *13*, 8731−8751. (c) Xiao, W.; Wang, X.; Liu, R.; Wu, J. Quinuclidine and its Derivatives as Hydrogen-Atom-Transfer Catalysts in Photoinduced Reactions. *Chin. Chem. Lett.* **2021**, *32*, 1847−1856. (d) Barham, J. P.;

Kaur, J. Site-Selective C(sp^3)-H Functionalizations Mediated by Hydrogen Atom Transfer Reactions via α-Amino/α-Amido Radicals. *Synthesis* **2022**, *54*, 1461−1477. (e) Aguilar Troyano, F. J.; Merkens, K.; Gómez-Suárez, A. Selectfluor® Radical Dication ($TEDA^{2+\cdot}$) - A Versatile Species in Modern Synthetic Organic Chemistry. *Asian J. Org. Chem.* **2020**, *9*, 992.

(13) Barham, J. P.; John, M. P.; Murphy, J. A. Contra-thermodynamic Hydrogen Atom Abstraction in the Selective C-H Functionalization of Trialkylamine N-CH_3 Groups. *J. Am. Chem. Soc.* **2016**, *138*, 15482−15487.

(14) Dimakos, V.; Su, H. Y.; Garrett, G. E.; Taylor, M. S. Site-Selective and Stereoselective C-H Alkylations of Carbohydrates via Combined Diarylborinic Acid and Photoredox Catalysis. *J. Am. Chem. Soc.* **2019**, *141*, 5149−5153.

(15) Ye, J.; Kalvet, I.; Schoenebeck, F.; Rovis, T. Direct α-Alkylation of Primary Aliphatic Amines Enabled by CO_2 and Electrostatics. *Nat. Chem.* **2018**, *10*, 1037.

(16) Xie, X.; Qiao, K.; Shao, B.-R.; Jiang, W.; Shi, L. Visible-Light-Promoted Radical Cross-Dehydrogenative Coupling of C(sp^3)-H/C(sp^3)-H and C(sp^3)-H/C(sp^2)-H via Intermolecular HAT. *Org. Lett.* **2023**, *25*, 4264−4269.

(17) Murray, P. R. D.; Cox, J. H.; Chiappini, N. D.; Roos, C. B.; McLoughlin, E. A.; Hejna, B. G.; Nguyen, S. T.; Ripberger, H. H.; Ganley, J. M.; Tsui, E.; Shin, N. Y.; Koronkiewicz, B.; Qiu, G.; Knowles, R. R. Photochemical and Electrochemical Applications of Proton-Coupled Electron Transfer in Organic Synthesis. *Chem. Rev.* **2022**, *122*, 2017−2291.

(18) Mayer, J. M. Bonds over Electrons: Proton Coupled Electron Transfer at Solid-Solution Interfaces. *J. Am. Chem. Soc.* **2023**, *145*, 7050−7064.

(19) Darcy, J. W.; Koronkiewicz, B.; Parada, G. A.; Mayer, J. M. A Continuum of Proton-Coupled Electron Transfer Reactivity. *Acc. Chem. Res.* **2018**, *51*, 2391−2399.

(20) Nocera, D. G. Proton-Coupled Electron Transfer: The Engine of Energy Conversion and Storage. *J. Am. Chem. Soc.* **2022**, *144*, 1069−1081.

(21) Warburton, R. E.; Soudackov, A. V.; Hammes-Schiffer, S. Theoretical Modeling of Electrochemical Proton-Coupled Electron Transfer. *Chem. Rev.* **2022**, *122*, 10599−10650.

(22) Gentry, E. C.; Knowles, R. R. Synthetic Applications of Proton-Coupled Electron Transfer. *Acc. Chem. Res.* **2016**, *49*, 1546−1556.

(23) Nguyen, L. Q.; Knowles, R. R. Catalytic C-N Bond-Forming Reactions Enabled by Proton-Coupled Electron Transfer Activation of Amide N-H Bonds. *ACS Catal.* **2016**, *6*, 2894−2903.

(24) Ganley, J. M.; Murray, P. R. D.; Knowles, R. R. Photocatalytic Generation of Aminium Radical Cations for C-N Bond Formation. *ACS Catal.* **2020**, *10*, 11712−11738.

(25) Bartling, H.; Eisenhofer, A.; König, B.; Gschwind, R. M. The Photocatalyzed Aza-Henry Reaction of *N*-Aryltetrahydroisoquinolines: Comprehensive Mechanism, $H^{\bullet}$- versus H^{+}-Abstraction, and Background Reactions. *J. Am. Chem. Soc.* **2016**, *138*, 11860−11871.

(26) Zhang, T.; Huang, H. Photocatalyzed Aminomethylation of Alkyl Halides Enabled by Sterically Hindered N-Substituents. *Angew. Chem., Int. Ed.* **2023**, *62*, No. e202310114.

(27) Le, C.; Liang, Y.; Evans, R. W.; Li, X.; MacMillan, D. W. C. Selective sp^3 C-H Alkylation via Polarity-Match-Based Cross-Coupling. *Nature* **2017**, *547*, 79−83.

(28) Wang, Y.; Carder, H. M.; Wendlandt, A. E. Synthesis of Rare Sugar Isomers through Site-Selective Epimerization. *Nature* **2020**, *578*, 403−408.

(29) Shaw, M. H.; Shurtleff, V. W.; Terrett, J. A.; Cuthbertson, J. D.; MacMillan, D. W. C. Native Functionality in Triple Catalytic Cross-Coupling: sp^3 C-H Bonds as Latent Nucleophiles. *Science* **2016**, *352*, 1304−1308.

(30) Maity, B.; Zhu, C.; Yue, H.; Huang, L.; Harb, M.; Minenkov, Y.; Rueping, M.; Cavallo, L. Mechanistic Insight into the Photoredox-Nickel-HAT Triple Catalyzed Arylation and Alkylation of α-Amino C_{sp3}-H Bonds. *J. Am. Chem. Soc.* **2020**, *142*, 16942−16952.

(31) Zhang, X.; MacMillan, D. W. C. Direct Aldehyde C-H Arylation and Alkylation via the Combination of Nickel, Hydrogen Atom Transfer, and Photoredox Catalysis. *J. Am. Chem. Soc.* **2017**, *139*, 11353−11356.

(32) Twilton, J.; Christensen, M.; DiRocco, D. A.; Ruck, R. T.; Davies, I. W.; MacMillan, D. W. C. Selective Hydrogen Atom Abstraction through Induced Bond Polarization: Direct a-Arylation of Alcohols through Photoredox, HAT, and Nickel Catalysis. *Angew. Chem., Int. Ed.* **2018**, *57*, 5369−5373.

(33) Barzanò, G.; Mao, R.; Garreau, M.; Waser, J.; Hu, X. Tandem Photoredox and Copper-Catalyzed Decarboxylative C(sp^3)-N Coupling of Anilines and Imines Using an Organic Photocatalyst. *Org. Lett.* **2020**, *22*, 5412−5416.

(34) Meng, Y.; Pan, C.; Liu, N.; Li, H.; Liu, Z.; Deng, Y.; Wei, Z.; Xu, J.; Fan, B. Photocatalytic Synthesis of 2,3-Diamines from Anilines and DIPEA via C-N Bond Cleavage and C-C Bond Formation. *Green Chem.* **2024**, *26*, 300−305.

(35) Beatty, J. W.; Stephenson, C. R. J. Amine Functionalization via Oxidative Photoredox Catalysis: Methodology Development and Complex Molecule Synthesis. *Acc. Chem. Res.* **2015**, *48*, 1474−1484.

(36) Xiao, W.; Zhang, J.; Wu, J. Recent Advances in Reactions Involving Carbon Dioxide Radical Anion. *ACS Catal.* **2023**, *13*, 15991−16011.

(37) Capaldo, L.; Quadri, L. L.; Ravelli, D. Photocatalytic Hydrogen Atom Transfer: the Philosopher's Stone for Late-Stage Functionalization? *Green Chem.* **2020**, *22*, 3376−3396.

(38) Zhou, C.; Lei, T.; Wei, X.-Z.; Ye, C.; Liu, Z.; Chen, B.; Tung, C.-H.; Wu, L.-Z. Metal-Free, Redox-Neutral, Site-Selective Access to Heteroarylamine via Direct Radical-Radical Cross-Coupling Powered by Visible Light Photocatalysis. *J. Am. Chem. Soc.* **2020**, *142*, 16805−16813.

(39) Ghosh, A.; Pyne, P.; Ghosh, S.; Ghosh, D.; Majumder, S.; Hajra, A. Visible-Light-Induced Metal-Free Coupling of C(sp^3)-H Sources with Heteroarenes. *Green Chem.* **2022**, *24*, 3056−3080.

(40) Tyson, E. L.; Niemeyer, Z. L.; Yoon, T. P. Redox Mediators in Visible Light Photocatalysis: Photocatalytic Radical Thiol-Ene Additions. *J. Org. Chem.* **2014**, *79*, 1427−1436.

(41) Li, H.; Guo, Y.; Wu, J.; Zhang, M. Proton-Coupled Electron Transfer Oxidation of O-H Bond by the N-Radical Cation of Wurster's Blue Salt ($TMPDA^{\bullet+}$). *Chem. Commun.* **2019**, *55*, 3465−3468.

(42) Naniwa, S.; Tyagi, A.; Yamamoto, A.; Yoshida, H. Visible-light Photoexcitation of Pyridine Surface Complex, Leading to Selective Dehydrogenative Cross-Coupling with Cyclohexane. *Phys. Chem. Chem. Phys.* **2018**, *20*, 28375−28381.

(43) Welker, E. A.; Tiley, B. L.; Sasaran, C. M.; Zuchero, M. A.; Tong, W.-S.; Vettleson, M. J.; Richards, R. A.; Geruntho, J. J.; Stoll, S.; Wolbach, J. P.; Rhile, I. J. Conformational Change with Steric Interactions Affects the Inner Sphere Component of Concerted Proton-Electron Transfer in a Pyridyl-Appended Radical Cation System. *J. Org. Chem.* **2015**, *80*, 8705−8712.

(44) Shen, G.-B.; Qian, B.-C.; Fu, Y.-H.; Zhu, X.-Q. Thermodynamics of the Elementary Steps of Organic Hydride Chemistry Determined in Acetonitrile and their Applications. *Org. Chem. Front.* **2022**, *9*, 6001−6062.

(45) Shen, G.-B.; Qian, B.-C.; Luo, G.-Z.; Fu, Y.-H.; Zhu, X.-Q. Thermodynamic Evaluations of Amines as Hydrides or Two Hydrogen Ions Reductants and Imines as Protons or Two Hydrogen Ions Acceptors, as Well as Their Application in Hydrogenation Reactions. *ACS Omega* **2023**, *8*, 31984−31997.

(46) Liu, W.-Z.; Bordwell, F. G. Gas-Phase and Solution-Phase Homolytic Bond Dissociation Energies of H-N^{+} Bonds in the Conjugate Acids of Nitrogen Bases. *J. Org. Chem.* **1996**, *61*, 4778−4783.

(47) Lai, W.; Li, C.; Chen, H.; Shaik, S. Hydrogen-Abstraction Reactivity Patterns from A to Y: The Valence Bond Way. *Angew. Chem., Int. Ed.* **2012**, *51*, 5556−5578.

https://doi.org/10.1021/acsomega.4c04209
ACS Omega 2024, 9, 26708−26718

(48) Zhang, J.-Y.; Wang, L.-L.; Zhu, X.-Q. Characteristic Activity Parameters of Electron Donors and Electron Acceptors. *ACS Phys. Chem. Au* **2023**, *3*, 358−373.
(49) Sviatenko, L. K.; Gorb, L.; Hill, F. C.; Leszczynski, J. Theoretical Study of Ionization and One-Electron Oxidation Potentials of N-Heterocyclic Compounds. *J. Comput. Chem.* **2013**, *34*, 1094−1100.
(50) Nicewicz, D. A.; Roth, H.; Romero, N. Experimental and Calculated Electrochemical Potentials of Common Organic Molecules for Applications to Single-Electron Redox Chemistry. *Synlett* **2015**, *27*, 714−723.
(51) Warren, J. J.; Tronic, T. A.; Mayer, J. M. Thermochemistry of Proton-Coupled Electron Transfer Reagents and Its Implications. *Chem. Rev.* **2010**, *110*, 6961−7001.
(52) Agarwal, R. G.; Coste, S. C.; Groff, B. D.; Heuer, A. M.; Noh, H.; Parada, G. A.; Wise, C. F.; Nichols, E. M.; Warren, J. J.; Mayer, J. M. Free Energies of Proton-Coupled Electron Transfer Reagents and Their Applications. *Chem. Rev.* **2021**, *122*, 1−49.
(53) Yang, Q.; Li, Y.; Yang, J.-D.; Liu, Y.; Zhang, L.; Luo, S.; Cheng, J.-P. Holistic Prediction of the pK_a in Diverse Solvents Based on a Machine-Learning Approach. *Angew. Chem., Int. Ed.* **2020**, *59*, 19282−19291.
(54) The pK_a(XH$^+$)$_D$ data are from a prediction platform. As you can see from the predicted Figures S1−S120 in the Supporting Information, the last column displays the experimental pK_a values determined in a lab. The prediction platform collected all the determined pK_a data from the published literature and automatically shown the experimental data along with the predicted results. All the 24 pK_a(XH$^+$)$_D$ data from Table S2 are from the prediction platform.
(55) Shen, G.-B.; Qian, B.-C.; Zhang, G.-S.; Luo, G.-Z.; Fu, Y.-H.; Zhu, X.-Q. Thermodynamics Regulated Organic Hydride/Acid Pairs as Novel Organic Hydrogen Reductants. *Org. Chem. Front.* **2022**, *9*, 6833−6848.
(56) Shen, G.-B.; Fu, Y.-H.; Zhu, X.-Q. Thermodynamic Network Cards of Hantzsch Ester, Benzothiazoline, and Dihydrophenanthridine Releasing Two Hydrogen Atoms or Ions on 20 Elementary Steps. *J. Org. Chem.* **2020**, *85*, 12535−12543.
(57) Nutting, J. E.; Rafiee, M.; Stahl, S. S. Tetramethylpiperidine N-Oxyl (TEMPO), Phthalimide N-Oxyl (PINO), and Related N-Oxyl Species: Electrochemical Properties and Their Use in Electrocatalytic Reactions. *Chem. Rev.* **2018**, *118*, 4834−4885.
(58) Leifert, D.; Studer, A. Organic Synthesis Using Nitroxides. *Chem. Rev.* **2023**, *123*, 10302−10380.
(59) Intelli, A. J.; Lee, R. T.; Altman, R. A. Peroxide-Initiated Hydrophosphinylation of gem-Difluoroalkenes. *J. Org. Chem.* **2023**, *88*, 14012−14021.
(60) Bryden, M. A.; Zysman-Colman, E. Organic Thermally Activated Delayed Fluorescence (TADF) Compounds Used in Photocatalysis. *Chem. Soc. Rev.* **2021**, *50*, 7587−7680.
(61) Teets, T. S.; Wu, Y.; Kim, D. Photophysical Properties and Redox Potentials of Photosensitizers for Organic Photoredox Transformations. *Synlett* **2022**, *33*, 1154−1179.
(62) Fu, Y.-H.; Shen, G.-B.; Wang, K.; Zhu, X.-Q. New Insights into the Actual H-Abstraction Activities of Important Oxygen and Nitrogen Free Radicals: Thermodynamics and Kinetics in Acetonitrile. *ACS Omega* **2022**, *7*, 25555−25564.
(63) Fu, Y.-H.; Jia, T.; Shen, G.-B.; Zhu, X.-Q. Quantitative Evaluation of H-Donating Abilities of C(sp^3)-H Bonds of Nitrogen-Containing Heterocycles in Hydrogen Atom Transfer Reaction. *RSC Adv.* **2023**, *13*, 16023−16033.
(64) Yang, J.-D.; Ji, P.; Xue, X.-S.; Cheng, J.-P. Recent Advances and Advisable Applications of Bond Energetics in Organic Chemistry. *J. Am. Chem. Soc.* **2018**, *140*, 8611−8623.
(65) Xue, X.-S.; Ji, P.; Zhou, B.; Cheng, J.-P. The Essential Role of Bond Energetics in C-H Activation/ Functionalization. *Chem. Rev.* **2017**, *117*, 8622−8648.

https://doi.org/10.1021/acsomega.4c04209
ACS Omega 2024, 9, 26708−26718